Available online at www.sciencedirect.com
SCIENCE DIRECT®
Biochemical Pharmacology 67 (2004) 337–351
Biochemical Pharmacology
www.elsevier.com/locate/biochempharm

Cell cycle arrest and autoschizis in a human bladder carcinoma cell line following Vitamin C and Vitamin K_3 treatment

James M. Jamison[a,*], Jacques Gilloteaux[b], M. Reza Nassiri[c], Meenakshi Venugopal[a,1], Deborah R. Neal[a], Jack L. Summers[a]

[a]*Department of Urology, College of Medicine, Northeastern Ohio Universities, Summa Health System/NEOUCOM, Akron, OH 44304, USA*
[b]*Department of Anatomy, American University of the Caribbean School of Medicine, Campus St. Maarten, M.E.I.O. Inc., Ponce de Leon Blvd 901, Suite #401, Coral Gables, FL 33135, USA*
[c]*Department of Pharmacology/Toxicology, Lake Erie College of Osteopathic Medicine (LECOM), Erie, PA 16509, USA*

Received 24 April 2003; accepted 25 August 2003

Abstract

Exponentially growing cultures of human bladder tumor cells (T24) were treated with Vitamin C (VC) alone, Vitamin K_3 (VK_3) alone, or with a VC:VK_3 combination for 1, 2, or 4 hr. Flow cytometry of T24 cells exposed to the vitamins for 1 h revealed a growth arrested population and a population undergoing cell death. Cells in G_1 during vitamin treatment arrested in G_1 while those in S phase progressed through S phase and arrested in G_2/M. DNA synthesis decreased to 14 to 21% of control levels which agreed with the percent of cells in S phase during treatment. Annexin V labeling demonstrated the majority of the cells died by autoschizis, but necrosis and apoptosis also were observed. Catalase treatment abrogated both cell cycle arrest and cell death which implicated hydrogen peroxide (H_2O_2) in these processes. Redox cycling of VC and VK_3 increased H_2O_2 production and decreased cellular thiol levels and DNA content, while increasing intracellular Ca^{2+} levels and lipid peroxidation. Feulgen staining of treated cells revealed a time-dependent decrease in tumor cell DNA, while electrophoresis revealed a spread pattern. These results suggest that Ca^{2+} disregulation activates at least one DNase which degrades tumor cell DNA and induces tumor cell death.

Keywords: Vitamin C; Vitamin K_3; Bladder carcinoma; Autoschizis; Cell cycle arrest; Flow cytometry

1. Introduction

The bladder is the most common site of neoplasm in the urinary system and accounts for approximately 29% of all urologic tumors [1]. In 2002, it is estimated that 56,500 new bladder cases would be diagnosed and 12,600 deaths would result from bladder cancer in the United States [2]. Because of the multifocal nature of these tumors, instillation therapy (flooding of the bladder with a solution of chemotherapeutic or immunostimulating agents) is a common practice. However, instillation therapy of bladder carcinomas often requires repeated application of antitumor agents over a period of several years. Unfortunately because of the dose-limiting toxicity of chemotherapeutic agents, resistance to neoplastic agents, and recurrence of the cancer, a cure has remained elusive for many cancer patients [3]. Therefore, there is a substantial need for new therapeutic options with favorable pharmacokinetics and pharmacodynamic parameters as well as a selective mechanism of action.

Due to their low systemic toxicity, several vitamins have been evaluated for their abilities to prevent or treat cancer [4]. Vitamins A, B_6, C, E, and K_3 have all demonstrated activity in the prevention or treatment of bladder cancer [5–8]. In addition, Lamm *et al.* [4] have demonstrated that oral administration of megadoses of Vitamins A, B_6, C, and E in conjunction with zinc markedly reduced tumor recurrence in patients with transitional cell carcinoma. This vitamin treatment was nontoxic and produced a greater reduction in the rate of tumor recurrence than

* Corresponding author. Tel.: +1-330-325-6468; fax: +1-330-325-0522.
E-mail address: jmj@neoucom.edu (J.M. Jamison).
[1] Present address: Shire Laboratories, Rockville, MD 20850, USA.

Abbreviations: VC, Vitamin C; VK_3, Vitamin K_3; H_2O_2, hydrogen peroxide; Ca^{2+}, calcium ion; CD_{50}, 50% cytopathic dose; CD_{90}, 90% cytopathic dose; ROS, reactive oxygen species; MDA, malondialdehyde.

0006-2952/$ – see front matter © 2003 Elsevier Inc. All rights reserved.
doi:10.1016/j.bcp.2003.08.040

BCG immunotherapy which is the gold standard for the treatment of superficial bladder cancer. To date, the mechanism(s) providing this protection have not been elucidated.

Vitamin C and Vitamin K_3 also exhibit antitumor activity against bladder cancer [8,9]. When Vitamin C and Vitamin K_3 are combined in a VC:VK_3 ratio of 100:1, the combination exhibits tumor-specific antitumor activity against human breast, oral epidermoid, and endometrial tumor cell lines at doses which are 10–50 times lower than when either vitamin is administered alone [10]. Additional studies using hepatoma-bearing mice as a model have shown that the VC:VK_3 combination alone exhibits antitumor activity [11]. In addition, the VC:VK_3 combination has been shown to be an effective chemosensitizer and radiosensitizer that induces little systemic or major organ pathology [11,12]. Studies conducted in our laboratory demonstrate that the VC:VK_3 combination exhibits synergistic antitumor activity against a panel of human urologic tumor cell lines and against human prostate cancer cells (DU145) which have been implanted into nude mice [13]. The results of more recent studies with the T24 human bladder cancer cell line [14–17], demonstrated that Vitamin C and Vitamin K_3 treatment induced cell death by autoschizis.

In the current study, the antitumor activity of VC, VK_3, and the VC:VK_3 combination against the T24 human bladder cancer cell line has been determined following a continuous or a 1-hr pulse exposure to the vitamins. The 1-hr pulse vitamin exposure has been performed in an attempt to simulate exposure of bladder cancer cells to the vitamins during instillation therapy (the chemotherapeutic agent typically resides in the bladder for 1 hr or less). Flow cytometry, histochemistry, and bioassays have been employed to elucidate vitamin-induced changes in cell cycle, cell viability, cellular DNA content and status and cellular thiol content.

2. Materials and methods

2.1. Cell culture

The human bladder carcinoma cell line T24 (Grade III/IV) was purchased from the American Type Culture Collection and cultured in Eagle's Minimum Essential Medium (MEM, Gibco) supplemented with 10% fetal bovine serum (FBS, Gibco) and 50 μg/mL of gentamicin sulfate (Sigma Chemical Co.). All incubations were performed at 37° and with 5% CO_2 unless other conditions are stated.

2.2. Vitamin preparation

Vitamin C (ascorbic acid) and menadione sodium bisulfite (VK_3) were purchased from Sigma Chemical Co. and were dissolved in culture medium MEM to create 8000 μM VC, 500 μM VK_3, and 8000 μM VC/80 μM VK_3 stock solutions. Photodegradation of the vitamins was prevented by preparing all vitamin solutions in a darkened lamina flow hood.

2.3. Cytotoxicity assay

The cytoxicity assay was performed using the microtetrazolium assay [MTT 3-(4,5-dimethylthiazol-2-yl)-2,5-diphenyl-diphenyltetrazolium bromide] assay as described previously [18]. Corning 96-well titer plates were seeded with tumor cells (5×10^3 per well) and incubated for 24 hr. Vitamin test solutions were serially diluted with media in twelve 2-fold dilutions. Each dilution was added to seven wells of the titer plates and co-incubated with the tumor cells for 1 hr or 5 days. Tumor cells exposed to vitamins for 1 hr were subsequently washed twice with PBS, overlain, with culture media and incubated for 5 days. After vitamin treatment and the incubation period, cytotoxicity was evaluated using the MTT assay. Following linear regression, the line of best fit was determined and the CD_{50} was calculated. The fractional inhibitory concentration index (FIC) was employed to evaluate synergism.

2.4. Flow cytometry

Determination of cell DNA content and ploidy were done according to our previously published procedure [19]. Titer dishes were seeded with 1.0×10^6 T24 cells suspended in MEM. Following 24 hr of incubation, the MEM was removed, the cells were washed twice with PBS and then overlain with 2 mL of MEM containing the vitamins at their CD_{90} (2032 μM Vitamin C, 20.32 μM Vitamin K_3, or 2032 μM Vitamin C/20.32 μM Vitamin K_3 combination). T24 cells served as sham-treated control cells. Human foreskin fibroblast cells served as diploid internal standard cells in flow cytometric studies. After a 1-hr incubation period with vitamins, the cultures were washed free of vitamin and overlaid fresh MEM. After 24 hr, the cells were harvested from the titer dishes and suspended in 0.1% NP-40 in a Tris–citrate solubilization buffer which contained propidium iodide (5 mg/mL) and 0.1% RNase A. Thirty minutes later, DNA ploidy and cell cycle analysis was performed on a Ortho Cytoron flow cytometer. The data from 2×10^4 cells were collected (when possible), stored, and analyzed using ModFit Cell Cycle Analysis.

2.5. Annexin–propidium iodide staining

Annexin–propidium iodide staining was performed using an Annexin V-Fluos staining kit (Boehringer Mannheim). Tumor cells (7.1×10^4) were seeded on 12 mm circular micro coverslips, incubated overnight and treated with the vitamins at their CD_{90} for 1, 2, or 4 hr. Subsequently, the vitamin solutions were removed and the cells were washed with PBS and incubated in binding buffer (10 mM

Hepes/NaOH, pH 7.4, 140 mM NaCl, 2.5 mM $CaCl_2$). Annexin V and propidum iodide were added to a final concentration of 1 μg/mL and incubated for 15 min in the dark at room temperature. Cells were analyzed using an Olympus BHS image capture system equipped with an Applied Cytovision program (Applied) [20].

2.6. Histology preparation and Feulgen staining

Circular coverslips were seeded with 1.0×10^5 cells and incubated for 24 hr. The cells were then overlaid for 1, 2, and 4 hr with 2 mL of MEM containing vitamins. Sham-treated T24 cells were overlaid with MEM for the same duration. All cells were washed twice with PBS, fixed for 1 hr in formalin at room temperature and then washed three times for 5 min per wash with PBS. The cells were left in PBS until Feulgen staining could be performed. Feulgen staining was performed using the method of De Tomasi [21] as described by Pearse [22].

2.7. Rate of DNA synthesis

DNA synthesis was evaluated using the method of Shevach [23]. T24 cells (1×10^6) were exposed for 1 hr to vitamins at their CD_{90} concentrations. Subsequently, they were washed twice with PBS and fresh media containing [^{3}H]-thymidine (1.0 μCi/mL) was added to the cells. After 4 hr, the media was removed and the cells were washed with PBS, soaked free from the monolayer with No-Zyme (JRH Biosciences). After an aliquot was removed for protein determination, the cells were harvested onto glass filters with a cell harvester. After the filters were air dried, they were mixed with scintillation cocktail and counted in a scintillation counter. Protein concentration was determined using the method of Bradford [24] and the data were expressed as counts per minute per microgram (cpm/μg) of protein. Sham-treated cells served as controls.

2.8. DNA fragmentation assay

Nucleosomal DNA degradation was assayed using the method of Sinha *et al.* [25]. Tumor cells were treated with the vitamins CD_{90} doses for 1, 2, 3, and 4 hr. Following the vitamin treatment, the cells were trypsinized, washed with ice-cold PBS, and resuspended at a density of 2×10^6 cells/mL in cell lysis buffer (5 mM Tris, pH 7.4, 5 mM EDTA, and 0.5% Triton X-100). After 2 hr on ice, the lysate was centrifuged at 27,000 *g* for 20 min. The supernatant was exposed to proteinase K for 1 hr at 50° and extracted with phenol–chloroform. The aqueous layer was treated with 0.13 M NaCl and the DNA was precipitated overnight at −20° with 2 vol. of ethanol. Following treatment with boiled bovine pancreatic RNase for 1 hr at 50°, the DNA concentration was determined spectroscopically and 10 μg per lane of DNA was loaded into the wells of 1.3% agarose gels. Electrophoresis was carried out for 3 hr at 10 mA with TBE buffer (89 mM Tris–HCl, 89 mM boric acid, and 2 mM EDTA, pH 8.0). A Hae III digest of X174 DNA was applied to the gel as markers. DNA was visualized by UV illumination of ethidium bromide-treated gels.

2.9. Hydrogen peroxide assay

Hydrogen peroxide was assayed by monitoring the oxidation of dihydrorhodamine 123 to rhodamine 123 by hydrogen peroxide [26]. Three million cells were incubated with 5 μM dihydrorhodamine 123 for 15 min. Vitamin solutions were prepared in PBS containing 20 mM glucose (PBSG) and incubated with the cells for 15, 30, 45, or 60 min. The cells were washed twice with 2 mL of PBS. One milliliter of PBSG was added and the cells were scraped off the culture dish, sonicated, centrifuged at 4° and 2000 *g* for 10 min and the cell lysates were stored on ice. The hydrogen peroxide in the lysate was measured fluorimetrically using an excitation wavelength of 500 nm and an emission wavelength of 536 nm. The protein content was determined using the method of Bradford [24]. The results were calibrated as described by Royall and Ischeropoulos [26] and expressed as nanomoles of hydrogen peroxide per milligram of protein. Values were corrected for the rate of spontaneous autooxidation of dihydrorhodamine 123. Experiments were run in parallel in the presence of 0.2 mg/mL catalase to demonstrate the specificity of the reaction. Sham-treated cells were employed as controls.

2.10. Protein thiol assay

Cellular thiols were assayed using the method of Nagelkerke *et al.* [28]. Culture dishes were seeded with 3 million cells. After 24 hr, the culture medium was removed and the cells were exposed for 1 hr to culture media containing the vitamins at their CD_{90}. The cells were then washed with PBS, overlaid with vitamin-free culture media, trypsinized at 1-hr interval for 6 hr and centrifuged for 5 min at $800 \times g$. The cell pellets were washed twice with 6.5% trichloroacetic acid and resuspended in 1 mL of 0.5 M Tris−HCl (pH 7.6). Subsequently, 50 μL of 10 mM of methanolic 5,5′-dithio-bis-(2-nitrobenzoic acid) (Ellman's Reagent) was added and the solution was incubated at room temperature. After 20 min, the solution was centrifuged for 5 min at 1000 rpm and the absorbance of the supernatant was measured at 412 nm. Data were expressed as micromolar thiols per milligram of protein, calculated on the basis of a reduced glutathione (GSH) standard curve. Sham-treated cells served as controls.

2.11. Lipid peroxidation assay

Lipid peroxidation was evaluated using the thiobarbituric acid (TBA) method [27]. T24 cells were treated and harvested as described in the thiol assay. After centrifugation, the cell pellets were resuspended in 6.0% TCA, mixed

with 1 mL of 0.25 N HCl containing 0.375% TBA and 15% TCA, heated in a water bath for 15 min at 95° and then allowed to cool. Following centrifugation, the supernatant was monitored fluorimetrically for MDA production using an excitation wavelength of 532 nm and an emission wavelength of 555 nm. Data were expressed as nanomolar MDA per milligram of protein, calculated on the basis of a MDA standard curve generated using 1,1,3,3-tetramethoxypropane.

2.12. Calcium flux assay

Calcium concentrations were assayed using the method of Scott *et al.* [29]. Four million T24 cells were suspended in 1 mL of calcium- and magnesium-free Hank's Balanced Salt Solution (HBSS) containing the CD_{90} doses of the vitamins and incubated for 15, 30, 45, and 60 min. Following incubation, the cell suspensions were treated with 100 μL of 390 μM arsenazo III (2,2′-[1,8-dihydroxy-3,6-disulpho-2,7-naphthalene-bis(azo)]-dibenzenearsonic acid). One hundred microliters of 130 μM carbonyl cyanide *p*-(trifluoromethoxy) phenylhydrazone (FCCP) was added to the cell suspension and the mitochondrial calcium release was recorded until no further change in absorbance was observed at 675–685 nm. Then 100 μL of a 195 mM solution of the calcium ionophore A23187 was added and the extramitochondrial calcium release was recorded until no further change in absorbance was observed at 675 and 685 nm. The linear range of the standard curve was used to express the calcium concentration as nanomoles of calcium per milligram of protein [30]. Sham-treated cells were used as controls.

2.13. Statistical analysis

Three-way ANOVA was performed using BMDP statistical software. In the three-way ANOVA, the two-way interactions were tested at the 0.005 level of significance, while all other effects were tested at the 0.0022 level of significance.

3. Results

3.1. Antitumor activity of the vitamins

Continuous vitamin treatment of the T24 cells (Fig. 1) resulted in 50% cytotoxic dose (CD_{50}) values of 1.492 ± 141 μM for VC alone and 13.1 ± 0.01 μM for VK_3 alone. When the vitamins are combined, the CD_{50}

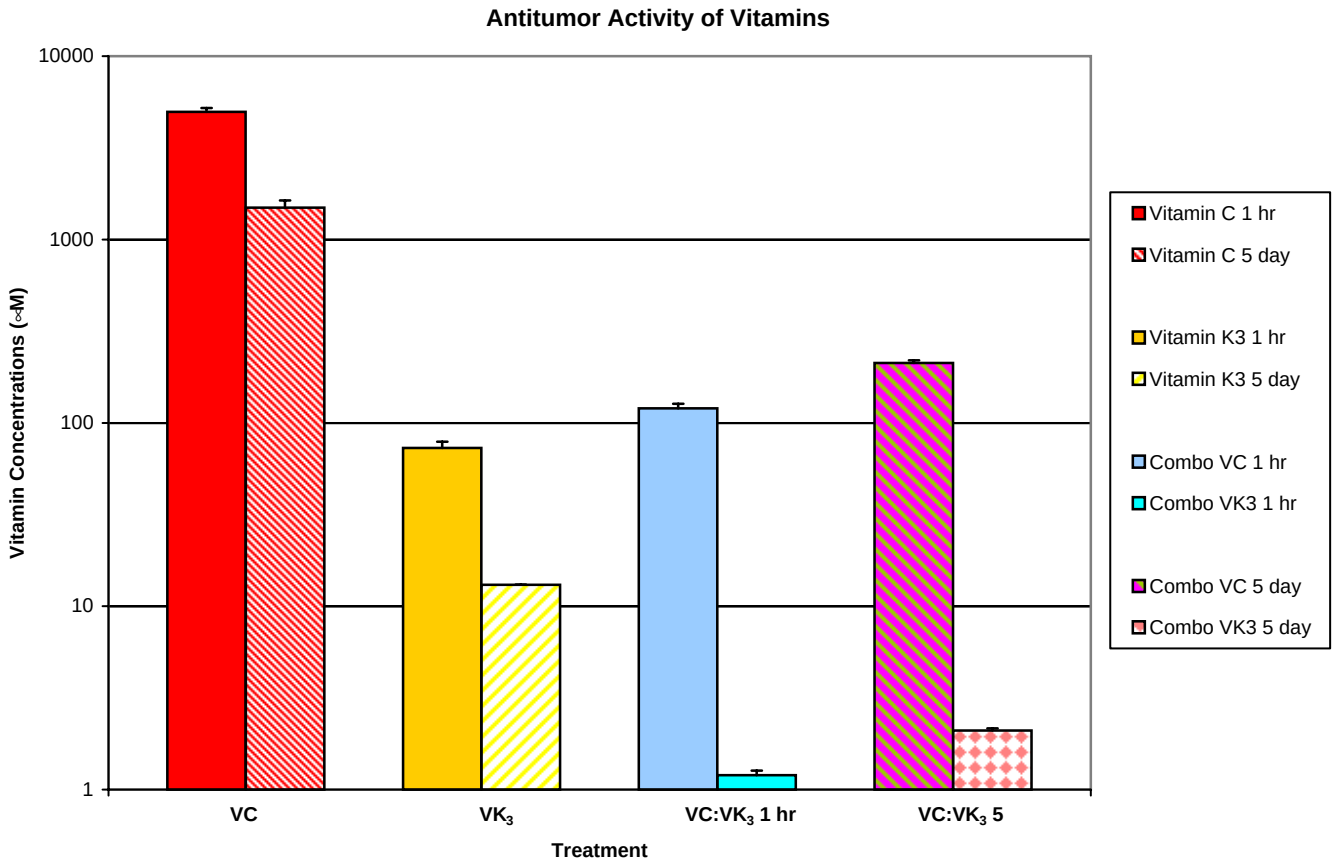

Fig. 1. Antitumor activity was measured by an MTT assay following a 5-day or 1-hr exposure to VC, VK_3, or a vitamin combination with a VC:VK_3 ratio of 100:1. Values are the mean ± SEM of three experiments with six readings per experiment. FIC = $CD_{50}^{A\,comb}/CD_{50}^{A\,alone} + CD_{50}^{B\,comb}/CD_{50}^{B\,alone}$, where $CD_{50}^{A\,alone}$ and $CD_{50}^{B\,alone}$ are 50% cytopathic doses of each vitamin alone; $CD_{50}^{A\,comb}$ and $CD_{50}^{B\,comb}$ are the 50% cytopathic doses of the vitamins administered together.

values of VC and VK_3 decrease to 212 ± 7.6 μM and 2.12 ± 0.06 μM, respectively. These results represent a 7-fold decrease in the CD_{50} of VC and a 6-fold decrease for VK_3. The FIC index has been used to evaluate the synergism of the vitamins. An FIC < 1.0 indicates the combination is synergistic, while an FIC > 1.0 indicates the combination is antagonistic. An FIC $= 1.0$ indicates the combination is indifferent. The FIC for continuously treated T24 cells is 0.158 which suggests the interaction between the vitamins is synergistic. One hour pulse treatment of the T24 cells with the vitamins resulted in CD_{50} values of 4.974 ± 246 μM for VC alone and 73.0 ± 5.9 μM for VK_3 alone. When the vitamins are combined, the CD_{50} values of VC and VK_3 decrease to 120 ± 7.0 μM and 1.20 ± 0.07 μM, respectively. These results represent a 41-fold decrease in the CD_{50} of VC and a 61-fold decrease for VK_3. The FIC for 1-hr treated T24 cells is 0.040 which suggests the interaction between the vitamins is very synergistic. The CD_{50} values of the vitamin-treated fibroblasts were 6-fold higher greater than they were for T24 cells (data not shown).

3.2. Vitamin effects on the tumor cell population

Flow cytometry was employed to determine whether vitamin treatment affects the cell cycle of T24 cells. Detached cells in the supernatant were pooled with adherent cells and then analyzed by flow cytometry. Human foreskin fibroblasts were mixed with T24 cells in an effort to determine the channel number of the true diploid G_0/G_1 peak (Fig. 2A). The true diploid peak (G_0/G_1 for the fibroblasts) is located in channel 59 while its corresponding G_2/M peak is located in channel 118. Conversely, the T24 cells exhibit a G_0/G_1 peak at channel 108 and a G_2/M peak in channel 214. These observations are in agreement with karyology studies which describe T24 cells as hypo- to hyper-tetraploid. In the case of sham treatment, 72% of the cells were in G_0/G_1, 18% were in S phase and 10% were in G_2/M.

Forward scatter of VC- and VC:VK_3-treated cells (data not shown) revealed the presence of two populations of cells. The first population (primarily the adherent cells) had the same dimensions as the sham-treated T24 cells, while the second population (primarily the detached cells) are smaller in size than the sham-treated T24 cells. The two populations also differ with respect to their DNA content with the detached cell population having less DNA than the adherent population. While these populations are seen as multiple peaks in these flow cytometry traces, the individual populations have been resolved by performing flow cytometry on the detached cells in the supernatant and the adherent cells separately (data not shown). In the case of VC treatment (Fig. 2B), 87% of the cells counted are adherent, aneuploid and the same size as control cells ($d = 30$–50 μm). This aneuploid population appears to be cycling and has a G_0/G_1 peak at channel 123 and a G_2/M peak at channel 244. Specifically, 36% of the cells in the aneuploid population were in G_0/G_1, 52% were in S phase and 12% were in G_2/M (Table 2). The remaining 13% of the cells counted are detached and of a smaller size than control cells (Table 1). Eighty-one percent of these cells were in G_0/G_1, while 19% were located in G_2/M compartment. The lack of cells in S phase suggests that either the cells are arrested in late G_1 phase or the cells are arrested in both G_1 and G_2/M and that the cells in G_1 are arrested in G_1 while those which have passed the G_1 checkpoint progress through S phase and become arrested in G_2/M. When the cell cycle distributions of both populations were calculated using weighted averages, 42% of the cells are in G_0/G_1 [$(81 \times 0.130) + (36 \times 0.87)$], 45% are in S phase, and 13% are in G_2/M (Table 3).

Table 1
Cell cycle distribution of the small T24 cells

Vitamin	G_0/G_1 phase	S phase	G_2/M phase
Vitamin C	81	0	19
Combination	79	47	20
Control	70	19	11

T24 cells were exposed to the vitamins at their 90% cytotoxic doses for 1 hr, incubated for 24 hr, and then harvested. DNA ploidy and cell cycle analysis was performed on an Ortho Cytoron flow cytometer and analyzed using ModFit Cell Cycle Analysis. Sham-treated T24 cells served as the negative control. Human foreskin fibroblasts served as diploid controls.

In the case of VK_3 treatment (Fig. 2C), 100% of the cells counted are adherent, aneuploid and of the same size as control cells ($d = 30$–50 μm). Fifty-two percent of the cells were in G_0/G_1, 28% were in S phase, and 20% were in G_2/M (Table 2). The substantial increase in the number of cells in S phase compared to sham-treated cells suggests that VK_3 may induce a late S phase or early G_2/M block in the cell cycle.

In the case of VC:VK_3 treatment (Fig. 2D), 47% of the cells counted were adherent, aneuploid and of the same size as control cells (Table 2). However, following VC/VK_3 treatment, 100% of the cells in the aneuploid population are blocked in late G_1 to early S phase. The remaining 53% of the cells counted were detached and of a smaller size than control cells (10–15 μm). Seventy-nine percent of these cells are in G_0/G_1, while 21% are in G_2/M (Table 1). As was the case for VC-treated cells, the lack of cells in S phase suggests that either the cells are arrested in late G_1 phase or the cells are arrested in both G_1 and G_2/M and that the cells in G_1 are arrested in G_1 while those which have

Table 2
Cell cycle distribution of the large T24 cells

Vitamin	G_0/G_1 phase	S phase	G_2/M phase
Vitamin C	36	52	12
Vitamin K_3	52	28	20
Combination	100	0	0
Control	72	18	10

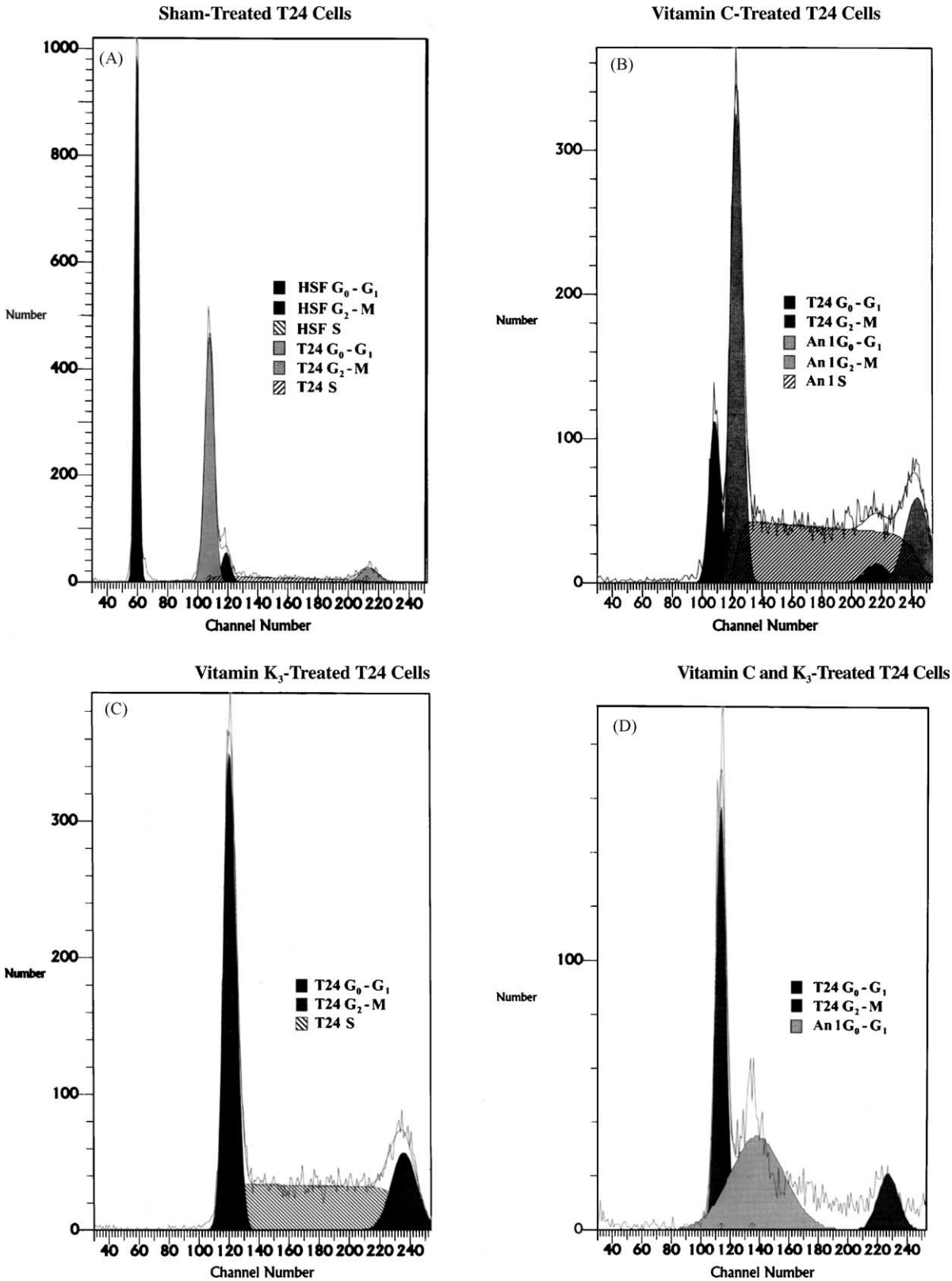

Fig. 2. T24 cells were exposed to the vitamins at their 90% cytotoxic doses for 1 hr. The vitamins were then removed, the cells were washed twice with PBS and the cells were overlain with culture medium. After 24 hr, the cells were harvested and DNA ploidy and cell cycle analysis was performed on an Ortho Cytoron flow cytometer. The data from 2×10^4 cells were collected (when possible), stored, and analyzed using ModFit Cell Cycle Analysis. Sham-treated T24 cells served as the negative control. Human foreskin fibroblasts served as diploid controls.

Table 3
Cell cycle distribution of the total T24 cells

Vitamin	G_0/G_1 phase	S phase	G_2/M phase
Vitamin C	42	45	13
Vitamin K_3	52	28	20
Combination	89	0	11
Control	70	19	11

passed the G_1 checkpoint progress through S phase and become arrested in G_2/M. When the cell cycle distributions of both populations are calculated using weighted averages, 89% of the cells are in G_0/G_1 [$(79 \times 0.530) + (47 \times 1.00)$] and 11% are in G_2/M (Table 3). Annexin V-FITC/PI labeling supported the data collected by flow cytometry. Co-incubation of T24 cells with an Annexin V-FITC/PI mixture following exposure of the cells to the vitamins revealed three populations of dying cells (Fig. 3) in addition to the cells which were growth arrested. The first population was dual-labeled oncotic cells. The second population was Annexin V-FITC-labeled apoptotic cells. The final population was minute, PI-labeled autoschizic cells. Light micrographs of sham-treated T24 cells revealed that less than 10% of the cells were undergoing cell death. Specifically, $1.6 \pm 0.4\%$ of the sham-treated cells were oncotic, $4.1 \pm 0.7\%$ were apoptotic and $2.9 \pm 0.4\%$ were autoschizic. In addition, $16.2 \pm 3.5\%$ of the Vitamin C-treated cells were undergoing autoschizis, while $4.6 \pm 0.7\%$ were apoptotic and $2.3 \pm 0.5\%$ were oncotic. In the case of VK_3-treated cells, $21.1 \pm 3.7\%$ of the cells were undergoing autoschizis, while $4.5 \pm 0.6\%$ were undergoing apoptosis and $2.7 \pm 0.3\%$ were oncotic. Finally, $29.3 \pm 5.5\%$ of the VC:VK_3-treated cells were undergoing autoschizis, while $4.6 \pm 0.8\%$ were apoptotic and $2.1 \pm 0.4\%$ were oncotic.

Light micrographs of sham (Sh)-treated bladder carcinoma T24 cells showed pleiomorphic cells with their long axis ranging between 30 and 35 μm and short axis ranging between 12 and 17 μm (Fig. 4, Sh2 and Sh4). Feulgen stain is seen as a reddish-purple which contrasts the large round, ovoid to subspherical nuclei with the gray, poorly contrasted cytoplasm. The smallest, postmitotic nuclei appeared more contrasted than the nuclei of the spread cells. After a 2-hr VC treatment (Fig. 4, VC2), T24 cells appeared flattened with lengths up to 35 μm and widths between 15 and 20 μm. The nuclei appear rounded and the Feulgen staining was less intense than in sham-treated T24

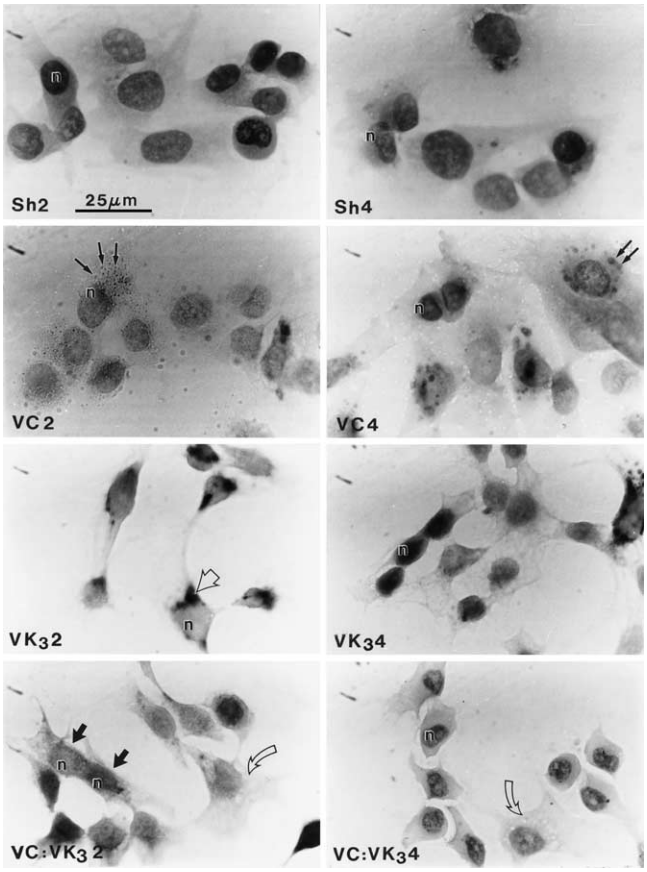

Fig. 4. Feulgen-stained T24 human bladder carcinoma cells illustrate 2-hr (Sh2) and 4-hr (Sh4) sham treatments, 2-hr VC2 and 4-hr VC4 treatments, 2-hr $VK_3$2 and 4-hr $VK_3$4 treatments and 2-hr VC:$VK_3$2 and 4-hr VC:$VK_3$4 treatments of T24 cells. In all the micrographs, 'n' represents the nucleus. Small dark arrows in VC2 and VC4 indicate the cytoplasmic localization of pigments. In $VK_3$2, the open arrow indicates Feulgen deposits in perikaryon. Thick, dark arrows in VC:$VK_3$2 indicate an example of doublet containing two nuclei. The curved arrows point toward areas of cytoplasm undergoing scission. The scale in Sh2 for all the illustrations is 25 μm.

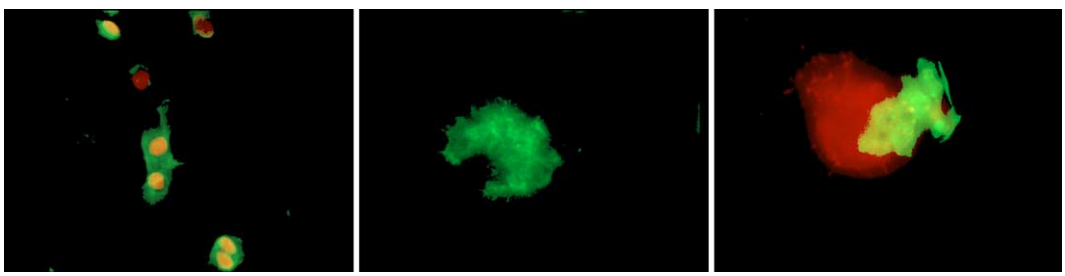

Fig. 3. T24 cells were exposed to the vitamins at their 90% cytotoxic doses for 1, 2, or 4 hr. Staining was performed using an Annexin V-Fluos staining kit. Annexin V-FITC and propidium iodide were added and incubated for 15 min. Three populations of dying cells were observed: dual-labeled (green membrane and red to orange nucleus) oncotic cells, Annexin V-FITC-labeled (green membranes) apoptotic cells, and PI-labeled (red to orange nucleus alone or with adherent pieces of yellow or green membrane) autoschizic cells. (For interpretation of the references to color in this figure legend, the reader is referred to the web version of this article.)

cells. Moreover, yellow-brown deposits ($d < 0.5$ μm) were also detectable in the cytoplasm. Following a 4-hr VC treatment (Fig. 4, VC4), some T24 cells still appeared to undergo mitosis. The peripheral regions of the cytoplasm acquired large brownish deposits ($d = 0.5$–1.5 μm) due to the fusion of small ones seen in Fig. 4 (VC2).

Following a 2-hr treatment with VK_3 (Fig. 4, VK_3), the cells ranged from 12 to 30 μm in length and from 8 to 13 μm in width and were interconnected through a network of bridging cell extensions. The intense extranuclear Feulgen stain demonstrated that DNA was being digested by lysosomal bodies. After 4 hr of VK_3 treatment, a few cells were dividing. However, most cells decreased to 15–20 μm in length and 11–13 μm in width and exhibited rounded nuclei smaller than those of control cells. Cytoplasmic Feulgen staining was less contrasted than in the control cells and contained bundles of fibrous material. A small number of cells contained Feulgen positive cytoplasmic granules that may represent intralysosomal DNA digestion (Fig. 4, $VK_3$4).

A 2-hr VC:VK_3 treatment (Fig. 4, VC:$VK_3$2) yielded fusiform cells which were 10–18 μm in length and 10–12 μm in width (approximately 2/3 to 1/2 the size of sham-treated cells). Feulgen staining was highly variable. Although some cells were dividing, cytoplasmic excision defects (including doublets) were also apparent. A doublet arises when a T24 cell separates into an anuclear, biconcave, subspherical portion and a spherical, nucleate portion that are connected by a cytoplasmic bridge [11] (Fig. 4, VC:$VK_3$2). After a 4-hr treatment (Fig. 4, VC:$VK_3$4), the cells were between 10 and 15 μm in length and between 8 and 12 μm in width (i.e. half the size of sham-treated cells). The Feulgen staining of the nuclei was significantly less intense than sham-treated cells. Many cells had detached from the coverslips, leaving a small number of doublets whose aneucleate half appeared smaller than the nucleate half (see Fig. 4, VC:$VK_3$2, dense arrows). Many of these cells showed cytoplasmic self excisions (Fig. 4, VC:$VK_3$4) and other morphological characteristic of autoschizis.

3.3. Effects of vitamin treatment on tumor DNA

The effect of vitamin treatment on the DNA synthesis of T24 cells has been assayed in an effort to determine if cells are arrested in late G_1 phase or if the cells are arrested in both G_1 and G_2/M and that the cells in G_1 are arrested in G_1 while those which have passed the G_1 checkpoint progress through S phase and become arrested in G_2/M (Fig. 5). VC and VK_3 treatment resulted in an 82% and a 79% reduction in the amount of thymidine incorporated, while the

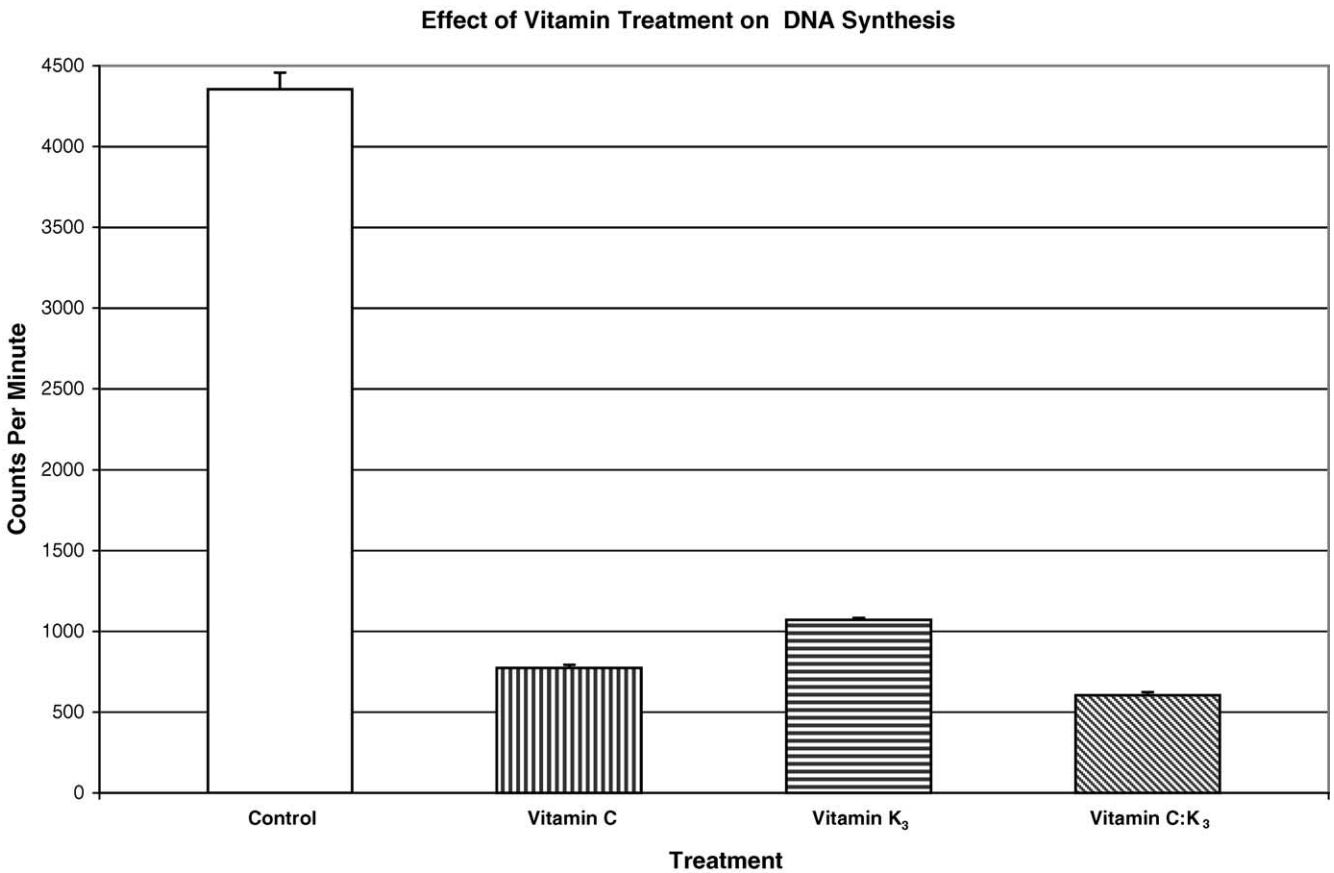

Fig. 5. Cultures of exponentially growing T24 cells were treated for 1 hr with the vitamins at their CD_{90} doses. After the vitamins were removed, the cultures were washed with PBS and exposed to 1 μCi/mL [^{3}H]-thymidine for 4 hr. The cells were then harvested onto glass filters and the amount of radioactivity incorporated was determined. The values represent the mean ± SD of three replicates and were compared to the control ($P < 0.005$).

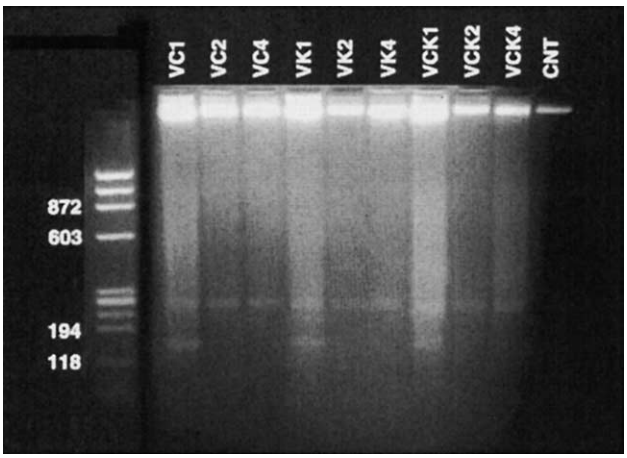

Fig. 6. Total DNA was extracted from T24 cells following sham treatment or 1, 2, or 4 hr treatment with VC, VK_3 or the vitamin combination and resolved electrophoretically. Lane 1 contains a Hae III digest of X174 DNA as a molecular weight marker. Lanes 2–4 contain the DNA of VC-treated T24 cells (VC1, VC2, VC4). Lanes 5–7 contain the DNA from VK_3-treated cells (VK1, VK2, VK4). Lanes 8–10 contain DNA from VC:VK_3-treated T24 cells (VCK1, VCK2, VCK4), while lane 11 contains the DNA of sham-treated cells. The DNA of all the vitamin-treated cells exhibits a spread pattern with treatment times as short as 1 hr. Conversely, the DNA from sham-treated cells (CNT, lane 11) appears as a high molecular weight band. Finally, faint, low molecular weight bands are seen at and below the 2 kb marker in vitamin-treated cells (lanes 2–10). These bands represent either contamination with rRNA or the presence of apoptotic cells in the predominately, autoschizic cell population.

VC:VK_3 combination produced an 86% decrease in thymidine incorporation. These results demonstrate a dramatic increase in the number of cells which are blocked in late G_1 phase, i.e. 89% for VC:VK_3 vs. 42% for VC alone. The dramatic decrease in the number of cycling cells could be due to a number of factors including DNase activation and subsequent DNA damage. The difference in the degree of enrichment of the small cell population in G_0/G_1 for VC:VK_3 vs. VC is a measure of the increase in autoschizic tumor cell death with the vitamin combination.

Total DNA was extracted from T24 cells following sham treatment or 1, 2, or 4 hr treatment with VC, VK_3, or the vitamin combination and was then resolved electrophoretically as shown in Fig. 6 in an effort to determine if the DNA was cleaved by the vitamin treatment. Lane 1 contains a molecular weight marker. Lanes 2–4 contain the DNA of VC-treated T24 cells (VC1, VC2, VC4). Lanes 5–7 contain the DNA from VK_3-treated cells (VK1, VK2, VK4). Lanes 8–10 contain DNA from VC:VK_3-treated T24 cells (VCK1, VCK2, VCK4), while lane 11 contains the DNA of sham-treated cells. The DNA of all the vitamin-treated cells exhibit a spread pattern with treatment times as short as 1 hr. Conversely, the DNA from sham-treated cells (CNT, lane 11) appears as a high molecular weight band. Finally, faint, low molecular weight bands are seen at and below the 2 kb marker in vitamin-treated cells (lanes 2–10). These bands represent either contamination with rRNA or the presence of apoptotic cells in the predominately, autoschizic cell population.

3.4. Hydrogen peroxide production and its effects on tumor cells

Previous studies have suggested that H_2O_2 generation is necessary for the antitumor activity of the vitamins [18,31,32]. In addition, low-level oxidative stress induced by H_2O_2 has been shown to induce cell cycle arrest in both G_1 and G_2/M phases of the cell cycle [33]. Therefore, vitamin-induced H_2O_2 formation was measured fluorimetrically in cell lysates at 15-min increment for 1 hr by evaluating the oxidation of dihydrorhodamine 123 to rhodamine 123 and expressed in terms of nanomoles of hydrogen peroxide per milligram of protein (Fig. 7). The intracellular H_2O_2 content of sham-treated T24 cells varied from 2.20 to 2.46 nmol with an average value of 2.36 ± 0.11 nmol. VC exposure resulted in an increase of H_2O_2 content to 20.80 ± 2.30 nmol during the first 15 min of incubation and to 36.40 ± 2.90 nmol during the second 15 min of incubation. The H_2O_2 content rapidly decreased to 11.00 ± 1.00 nmol during the next 15 min and remained constant during the final 15 min of incubation. VK_3 treatment increased H_2O_2 content to 8.17 ± 0.40 nmol during the first 15 min of incubation and to 19.80 ± 1.40 nmol during the second 15 min of incubation. The H_2O_2 content remained constant during the next 15 min and decreased slightly to 15.10 ± 2.40 nmol H_2O_2 during the final 15 min of incubation. Following VC:VK_3 treatment, H_2O_2 levels increased to 5.90 ± 2.34 nmol during the first 15 min of incubation and then rose to 9.30 ± 1.14 nmol during the second 15 min of incubation. The H_2O_2 content gradually decreased during the final 30 min of incubation to 5.00 ± 0.79 nmol. In all cases, the antitumor activity was abrogated by the addition of exogenous catalase.

Since exposure of tumor cells to the vitamins is known to result in the generation of H_2O_2 and that may initiate membrane lipid peroxidation [10,31,34]. The effect of vitamin treatment on cellular lipid peroxidation (Fig. 8) has been examined by exposing the cells to the vitamins for 1, 2, 3, 4, or 5 hr and then using the thiobarbituric acid method [27]. All lipid peroxidation data are presented as micromolar MDA per milligram of protein. The lipid peroxidation of sham-treated T24 cells varied from 8.13 to 9.45 μM with an average value of 9.17 ± 0.22 μM. However, this is only a measure of the lipid peroxidation that occurs during the heating of samples to 95° during the assay and can, therefore, be considered as a baseline for MDA production. VC exposure increased MDA production to 12.60 ± 0.50 μM during the first hour and the MDA levels remained constant for the next 2 hr. Subsequently, MDA levels rose to 57.90 ± 0.40 μM by the fourth hour and to 64.40 ± 0.60 μM during the final hour. VK_3 treatment increased MDA levels to 14.70 ± 0.70 μM during the first hour and they remained constant for the next 2 hr. MDA levels rose to 54.60 ± 1.00 μM by the fourth hour and remained constant for the final hour. The VC:VK_3 combination produced an increase in MDA concentration

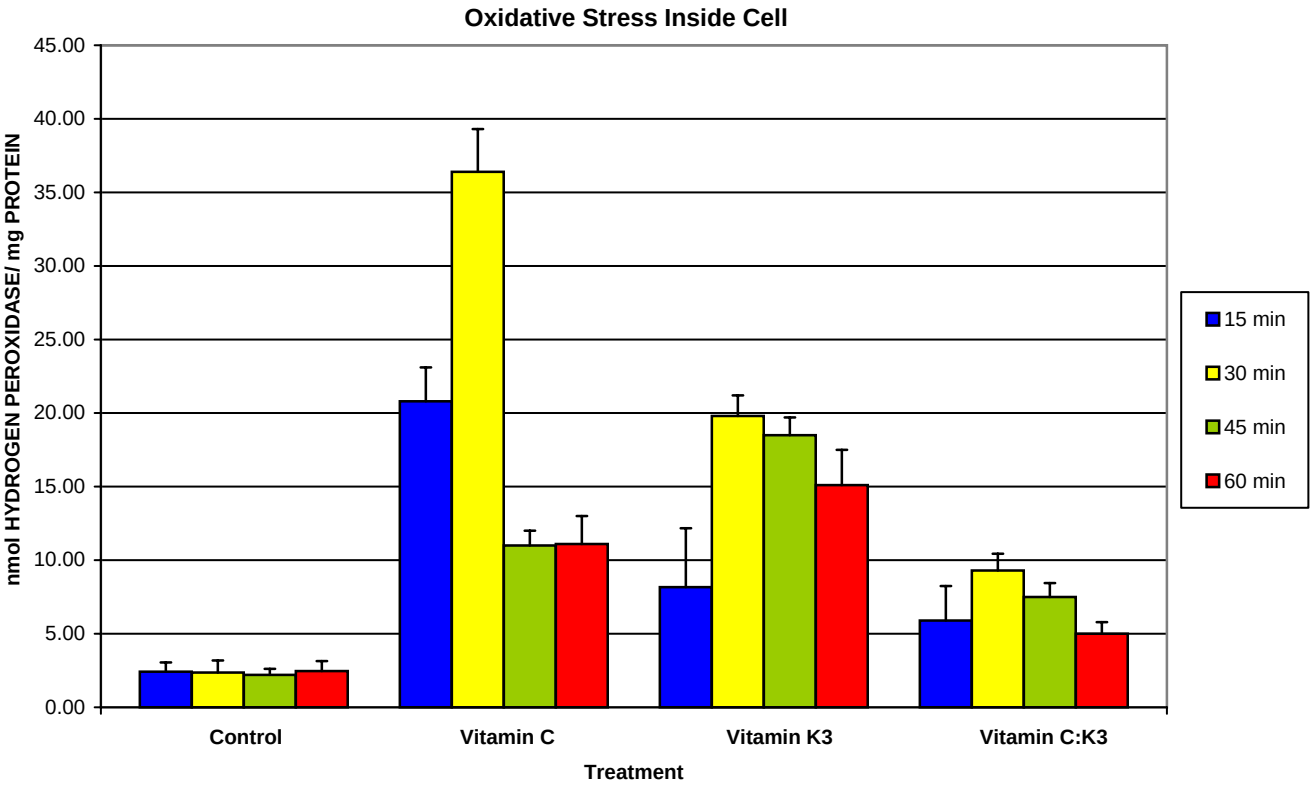

Fig. 7. Cultures of exponentially growing T24 cells were treated for 15, 30, 45, and 60 min with the vitamins at their CD_{90} doses. Hydrogen peroxide production was evaluated by monitoring the oxidation of dihydrorhodamine 123 to rhodamine 123. The results are expressed as the mean ± SEM of three experiments with three readings per experiment and were compared to control ($P < 0.005$).

to 16.70 ± 0.20 μM during the first hour. The MDA concentration decreased slightly by the second hour and remained constant for the third hour. MDA levels rose to 61.80 ± 1.20 μM by fourth hour and decrease slightly to 53.00 ± 0.80 μM during by the fifth hour. These results suggested lipid peroxidation was a late event in the cell death process.

3.5. Cellular thiol levels

Because administration of VK_3 to hepatocytes is known to induce a variety of effects including depletion of glutathione (GSH) and oxidation of protein sulfhydryl groups in cytoskeletal proteins [31,32,35,36], the effect of vitamin treatment on cellular thiols was examined following a 1, 2, 3, 4, or 5 hr vitamin exposure. All thiol data are presented as micromolar thiol per milligram of protein. The thiol content of sham-treated T24 cells varied from 1.37 to 1.45 μM with an average value of 1.39 ± 0.04 μM (Fig. 9). VC exposure resulted in a decrease in cellular thiol levels to 0.32 ± 0.02 μM (below control levels) during the first hour and remained constant for the second hour. Thiol levels rose gradually to 0.68 ± 0.05 μM by the third hour, decreased slightly to 0.55 ± 0.14 μM during the fourth hour and remained constant during the final hour. VK_3 treatment lowered thiol levels to 0.56 ± 0.06 μM during the first hour and to 0.24 ± 0.02 μM by the second hour. Thiol levels increased to 0.47 ± 0.03 μM by the third hour and remained near this level for the final 2 hr. The VC:VK_3 combination produced a decrease in thiol concentration to 0.32 ± 0.01 μM during the first hour. Thiol levels increased to 0.49 ± 0.20 μM by the second hour and vacillated between 0.51 ± 0.03 μM and 0.72 ± 0.02 μM during the final 3 hr.

3.6. Cellular calcium fluxes

The presence of H_2O_2 can induce Ca^{2+} fluxes within the tumor cells which can mediate activation of transcription factors, cell cycle arrest and even cell death [37]. Therefore, vitamin-induced fluxes in cellular calcium (Table 4) were measured using the arsenazo III method of Bellomo and coworkers [38,39]. Experiments were performed in the presence or absence of A23187 so that the effect of the vitamins on the calcium levels in both the mitochondrial (MC) and extramitochondrial (EMC) compartments could be determined and expressed in nanomoles of calcium per milligram of protein. The mitochondria of sham-treated T24 cells contained an average Ca^{2+} content of 6.84 ± 0.39 nmol, while the EMC contained an average Ca^{2+} content of 7.89 ± 0.32 nmol. VC treatment caused a rapid decrease of MC Ca^{2+} to 2.74 ± 0.42 nmol within 15 min and a gradual decrease to 0.53 ± 0.17 nmol during the next 15 min. VK_3 treatment decreased MC Ca^{2+} levels

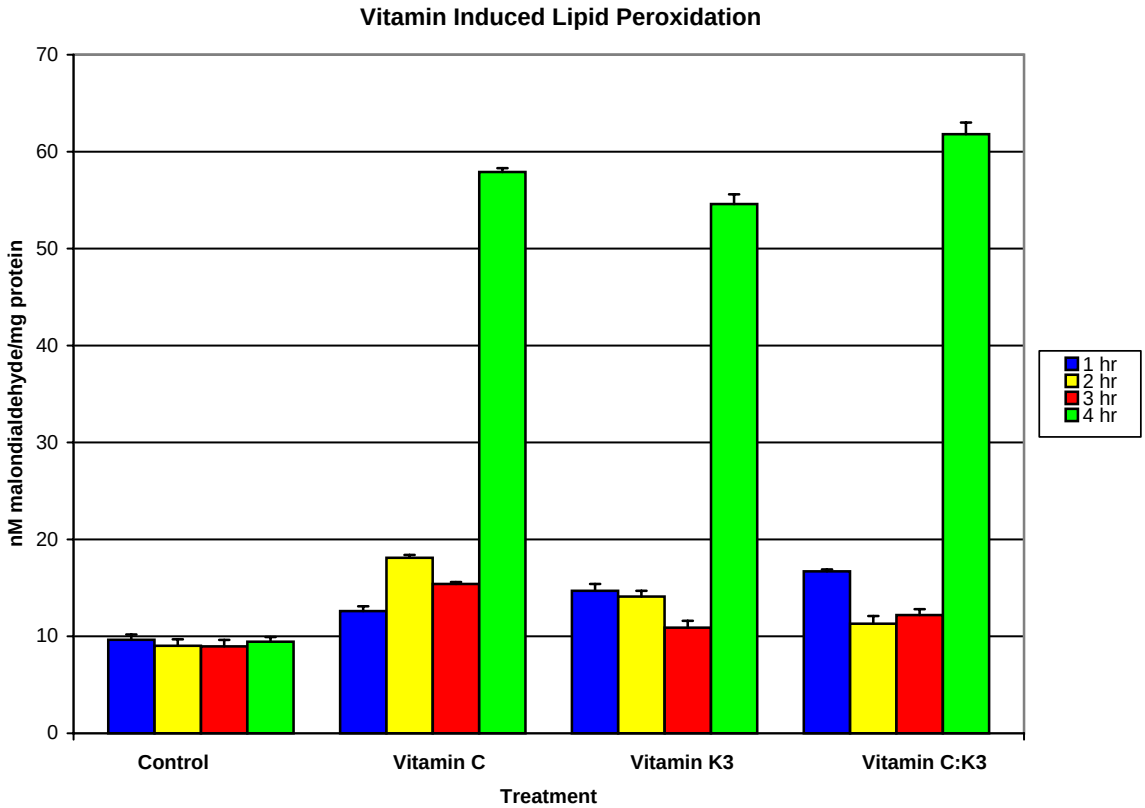

Fig. 8. T24 cells were treated for 1 hr with the vitamins at their CD_{90} doses, harvested at 1-hr interval for 5 hr and assayed for lipid peroxidation using the thiobarbituric acid method MDA production was monitored fluorimetrically and data were expressed as nanomolar MDA per milligram of protein, calculated on the basis of a MDA standard curve. Values are the mean ± SEM of three experiments with three readings per experiment and were compared to the control ($P < 0.005$).

to 1.18 ± 0.24 nmol within 30 min. MC Ca^{2+} levels increased to 2.00 ± 0.42 nmol during the next 15 min and then decreased to 1.49 ± 0.30 nmol. Combined vitamin treatment a rapid decrease in MC Ca^{2+} levels to 3.57 ± 0.35 nmol during the first 15 min and a gradual decrease to 1.75 ± 0.13 nmol over the next 45 min. VC treatment decreased EMC Ca^{2+} levels to 2.31 ± 0.21 nmol within 30 min and gradually decreased EMC Ca^{2+} to

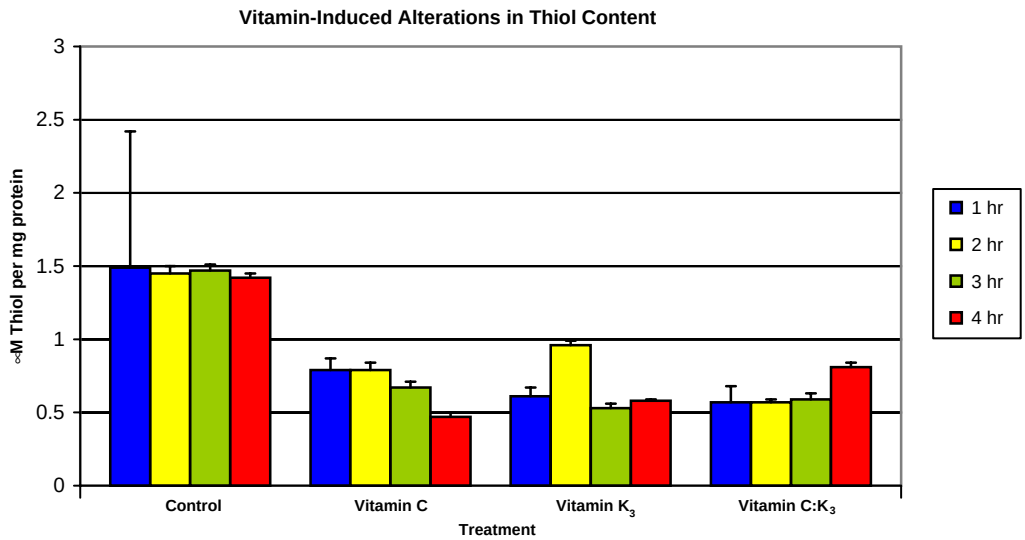

Fig. 9. Cultures of exponentially growing T24 cells were treated for 1 hr with the vitamins at their CD_{90} doses. The cells were harvested at 1-hr interval for 5 hr and cellular thiol content was assayed by monitoring absorbance at 412 nm following reaction with Ellman's Reagent. Data have been expressed as micromolar thiol per milligram of protein, calculated on the basis of an reduced glutathione standard curve. Values are the mean ± SEM of three experiments with three readings per experiment and were compared to the control ($P < 0.005$).

Table 4
Effect of vitamin treatment on calcium levels in T24 cells

Time (min)	Control		Vitamin C		Vitamin K_3		Combination	
	MC	EMC	MC	EMC	MC	EMC	MC	EMC
15	6.84 ± 0.39	7.89 ± 0.31	2.74 ± 0.42	4.44 ± 0.59	1.81 ± 0.17	2.94 ± 0.35	3.57 ± 0.33	3.80 ± 0.45
30	7.74 ± 0.93	8.52 ± 0.68	1.81 ± 0.15	2.31 ± 0.21	1.18 ± 0.24	2.44 ± 0.12	2.90 ± 0.28	3.40 ± 0.28
45	6.31 ± 0.68	7.95 ± 0.83	1.30 ± 0.05	1.81 ± 0.20	2.00 ± 0.42	1.53 ± 0.21	2.37 ± 0.24	1.24 ± 0.31
60	6.71 ± 0.72	8.19 ± 0.44	0.53 ± 0.17	1.39 ± 0.46	1.49 ± 0.30	2.65 ± 0.49	1.75 ± 0.13	1.35 ± 0.36

Calcium content of the mitochondrial (MC) and extramitochondrial (EMC) compartments were evaluated using the change in absorbance arsenazo III at 675 and 685 nm following exposure of T24 cells to the vitamins at their CD_{90} doses. FCCP was added to the cell suspension and mitochondrial calcium release was observed until there was no further change in absorbance. Subsequently, A23187 (an ionophore) was added to the cell suspension and extramitochondrial calcium release was recorded. Data are expressed as nanomoles of calcium per milligram of protein, calculated on the basis of a calcium standard curve. The results are expressed as the mean ± SEM of three experiments with three readings per experiment and were compared to the control ($P < 0.005$).

1.39 ± 0.46 nmol over the final 30 min. VK_3 treatment decreased EMC Ca^{2+} levels to 2.94 ± 0.26 nmol by 15 min. The EMC Ca^{2+} levels gradually decreased to 1.53 ± 0.21 nmol over the next 30 min and rose to 2.65 ± 0.49 over the final 15 min. Combined vitamin treatment decreased EMC Ca^{2+} levels to 3.80 ± 0.45 nmol min. The EMC Ca^{2+} levels decreased to 1.24 ± 0.31 nmol over the next 30 min and remained constant for the final 15 min.

4. Discussion

4.1. Cell cycle arrest

The results of the current study agree with the results of previous work conducted with other tumor cell lines [13,18,40,41]. When T24 or four other human bladder tumor cell lines are exposed to VC, VK_3, or the VC:VK_3 combination for 1 hr or a continuous 5 day exposure, the CD_{50} values for the vitamin combination for the 1 h vitamin exposure are essentially identical to the CD_{50} values for the vitamin combination for the continuous 5 day vitamin treatment. These observations suggest that changes in the cells during the first hour of treatment predispose the tumor cells to die. Flow cytometry of T24 cells treated with the vitamins for 1 hr and then incubated in vitamin-free culture medium for 24 hr reveal a growth arrested population and a population undergoing cell death. Cells that are in G_1 at the time of vitamin treatment are arrested in G_1, while those which have passed the G_1 checkpoint progress through S phase and become arrested in G_2/M. This dual cell cycle arrest appears to be due to the combined effects of H_2O_2 and the vitamins.

The *p53*, *p21* and *Rb* gene products have all been implicated in the H_2O_2-induced G_1 arrest [42–44], while regulation of cyclin B1 and $p34^{cdc2}$ are believed to be involved in the G_2/M arrest [33]. Furthermore, addition of VC to cells during oxidative stress, results in partial G_2/M cell cycle arrest and incomplete DNA repair in conjunction with increased intracellular oxidative stress, reduced intracellular GSH levels and increased cytotoxicity [45,46]. These results are consistent with those of other studies [34,47,48] that indicate VC can act as a pro-oxidant at elevated concentrations and induce the formation of H_2O_2. Finally, VK_3 is known to bind to the catalytic domain of Cdc25 phophatase that results in the formation of an inactive hyperphosphorylated Cdk1. In addition, VK_3 inhibits cyclin E expression at late G_1 phase and cyclin A expression at the G_1/S transition. Together these effects were shown to cause cell cycle arrest [49–51].

Flow cytometry of sham-treated cells indicate that approximately 13% of cells are in S phase. Since cells in S phase during vitamin treatment progress through S phase and thus synthesize DNA, one would expect the DNA synthesis rates of vitamin-treated cells in the tritiated thymidine incorporation assay to be approximately 13%. In fact, the DNA synthesis rate varies from 14 to 21% in vitamin-treated cells. The fact that cells arrested in G_1 do not undergo DNA repair may explain the chemosensitizing and radiosensitizing effects of the vitamin combination [11,12,52].

4.2. Cell death by autoschizis

Following a 1-hr exposure to VC:VK_3, 53% of the cells undergo cell death. If the time of VC:VK_3 exposure is increased, the amount of cell death also increases until all the cells are dead by 5 hr. As was the case in previous studies and for cell cycle arrest in the current study, addition of catalase abrogated cell death and implicated H_2O_2 in the cell cycle arrest death processes [10,18,40].

T24 and other tumor cell lines treated with the VC:VK_3 combination die by autoschizis which has been described in great detail in previous studies [14–16,40,41]. Ultrastructural studies of vitamin-treated tumor cells undergoing autoschizis revealed exaggerated membrane damage and an enucleation process in which the perikarya separated from the main cytoplasmic body by self-excision. These self-excisions continued until all that remained was an intact nucleus surrounded by a narrow rim of cytoplasm that contained damaged organelles. The nucleus exhibited nucleolar segregation and chromatin decondensation followed by nuclear karryohexis and karyolysis [14–16,40,41].

While the mechanism of action of these vitamins has not been elucidated completely, their autoschizic activity has been attributed to redox cycling of the vitamins and the possible generation of peroxides and other ROS followed by membrane lipid alteration, DNase activation, and DNA destruction by the Vitamin C and Vitamin K_3 combination in the catalase-deficient cancer cells [16,18,40,41,53].

While VC is traditionally perceived as an antioxidant [54], it may also act as a pro-oxidant and increase DNA damage and induce cell death [46,55]. Vitamin K_3 is an oxidant that exhibits antitumor activity against a variety of tumor cell lines as well as human explants which are resistant to other types of chemotherapy [29,30]. When VC is combined with VK_3, the interaction fosters single-electron reduction to produce the long-lived semiquinone and ascorbyl radical and increases the rate of redox cycling of the quinone [56,57] to form H_2O_2 and other ROS. Measurement of oxidative stress with dihydrorhodamine 123, indicates the rapid production of H_2O_2 and ROS by the vitamins. Within the first hour following vitamin treatment, this oxidative stress decreases cellular thiol levels to less than half those of sham-treated cells. This loss of protection against ROS is accompanied by the oxidation and subsequent disruption of cellular caspases (including caspase-3) as well as microtubules and other cytoskeletal proteins [40,41,58–61]. This cytoskeletal disorganization is reflected by blister and bleb formation as well as by acute distortions in tumor cell shape [36,62].

Because vitamin administration induces H_2O_2 production, the amount of lipid peroxidation, intracellular Ca^{2+} levels, and cellular DNA status have been evaluated. While the increase in lipid peroxidation values for cells are significantly higher than control levels after 1 hr of vitamin exposure, significant levels of lipid peroxidation and damage to the cell membrane occur only after 2–3 hr vitamin exposure and suggest lipid peroxidation is a late event in the cell death process. However, TEM micrographs demonstrated that mitochondrial architecture is rapidly altered by vitamin-induced lipid peroxidation and may be involved in the triggering mechanism of autoschizis [14–16]. As a consequence of the peroxidation, Ca^{2+} transport systems of the mitochondria, SER and plasma membrane are damaged and there is an increase in intracellular Ca^{2+} levels. Ca^{2+} disregulation leads to the exposure of phosphatidylserine (PS) on the outer surface of the plasma membrane and the activation a number of phospholipases, proteases, and DNases [63]. Co-incubation of T24 cells with an Annexin V-FITC/PI cocktail following vitamin exposure reveals three populations of cells: dual labeled cells necrotic cells, Annexin labeled cells apoptotic cells and propidium labeled autoschizic cells which predominate [40].

Since Ca^{2+} disregulation is known to activate DNases, the status of tumor cell DNA following vitamin treatment has been assessed [63]. Feulgen staining illustrates a time-dependent decrease in tumor cell DNA content which is due in part to the decreased rate of DNA synthesis and in part to the degradation of DNA by DNases. Electrophoretic analysis of DNA of vitamin-treated tumor cells reveals a spread pattern instead of the ladder pattern characteristic of apoptosis. *In vivo* data collected from implanted DU145 tumors indicate this spread pattern is the result of the caspase-3-independent, sequential reactivation of deoxyribonuclease I and II [63,64]. Due to the vitamin-induced decrease in cellular thiol levels, the increased ROS production is accompanied by the oxidation and subsequent disruption of microtubular and other cytoskeletal proteins [35,36,64]. Taken together these results indicate that autoschizis entails the coordinated attack of ROS and other species on cellular thiols, membranes, cytoskeleton, and DNA that continues until cell death by self-morsellation ensues. Since additional studies have shown that the $VC:VK_3$ combination is an effective chemosensitizer and radiosensitizer that induces little systemic or major organ pathology [11,12,40], we believe the selective antineoplastic effects of Vitamin C and Vitamin K_3 merit further investigation for clinical use.

Acknowledgments

This study was supported by the American Institute for Cancer Research, Washington, DC, Summa Health System Research Foundation, Akron, OH. We would like to thank Dr. H. Lorimer for use of the laboratory in the Department of Biological Sciences at Youngstown State University.

References

[1] Lynch F, Cohen MB. Urinary System. Cancer 1995;75:316–29.
[2] Jemal A, Thomas A, Murray T, Thun M. Cancer statistics, 2002. CA Cancer J Clin 2002;52:23–47.
[3] Kamat AM, Lamm DL. Chemoprevention of urological cancer. J Urol 1999;161:1748–60.
[4] Lamm DL, Riggs DR, Shriver JS, vanGilder PF, Rach JF, DeHaven JI. Megadose vitamins in bladder cancer: a double-blind clinical trial. J Urol 1994;151:21–6.
[5] Malone WF, Kelloff GJ, Pierson H, Greenwald P. Chemoprevention of bladder cancer. Cancer 1987;60:650–7.
[6] Lamm DL, Allaway M. Current trends in bladder cancer treatment. Ann Chir Gynaecol 2000;89:234–41.
[7] Marrian DH, Mitchell JS, Bull CH, King EA, Szaz KF. Labelled compound related to synkavit and its uptake in certain human tumours studied by radio-isotope scanning. Acta Radiol Ther Phys Biol 1969;8:221–46.
[8] Chlebowski RT, Dietrich M, Akman SA, Block JB. Vitamin K_3 (Menadione) inhibition of human tumor growth in the soft agar assay system. Proc ASCO 1984;3:93.
[9] Schlegel JU. Proposed use of ascorbic acid in the prevention of bladder carcinoma. Ann NY Acad Sci 1975;258:432–7.
[10] Noto V, Taper HS, Jiang YH, Janssens J, Bonte J, De Loecker W. Effects of sodium ascorbate (Vitamin C) and 2-methyl-1,4-naphthoquinone (Vitamin K_3) treatment on human tumor cell growth *in vitro*. I. Synergism of combined Vitamin C and K_3 action. Cancer 1989;63:901–6.

[11] Taper HS, de Gerlache J, Lans M, Roberfroid M. Non-toxic potentiation of cancer chemotherapy by combined C and K_3 vitamin pretreatment. Int J Cancer 1987;40:575–9.
[12] Taper HS, Keyeux A, Roberfroid M. Potentiation of radiotherapy by nontoxic pretreatment with combined Vitamins C and K_3 in mice bearing solid transplantable tumor. Anticancer Res 1996;16: 499–504.
[13] Jamison JM, Gilloteaux J, Taper HS, Summers JL. Evaluation of the *in vitro* and *in vivo* antitumor activities of Vitamin C and K3 combinations against human prostate cancer. J Nutr 2001;131:158S–60S.
[14] Gilloteaux J, Jamison JM, Arnold D, Ervin E, Eckroat L, Docherty JJ, Neal D, Summers JL. Cancer cell necrosis by autoschizis: synergism of antitumor activity of Vitamin C:Vitamin K_3 on human bladder carcinoma T24 cells. Scanning 1998;20:564–75.
[15] Gilloteaux J, Jamison JM, Arnold D, Summers JL. Autoschizis: another cell death for cancer cells induced by oxidative stress. Ital J Anat Embryol 2001;106:79–91.
[16] Gilloteaux J, Jamison JM, Arnold D, Taper HS, Summers JL. Ultrastructural aspects of autoschizis: a new cancer cell death induced by the synergistic action of ascorbate/menadione on human bladder carcinoma cells. Ultrastruct Pathol 2001;25:183–92.
[17] Ervin E, Jamison JM, Gilloteaux J, Docherty JJ, Summers JL. Characterization of the early events in Vitamin C and K_3-induced death of human bladder tumor cells. Scanning 1998;20:210–1.
[18] Venugopal M, Jamison JM, Gilloteaux J, Koch JA, Summers M, Giammar D, Sowick C, Summers JL. Synergistic antitumor activity of Vitamins C and K_3 on human urologic tumor cell lines. Life Sci 1996;56:1389–400.
[19] Nassiri MR, Hudson JL, Pudlo JS, Birch GM, Townsend LB, Drach JC. Flow cytometric evaluation of the cytotoxicity of novel antiviral compounds. Cytometry 1990;1:411–7.
[20] Vermes I, Clemens H, Steffens-Nakken H, Reutlingsperger C. A novel assay for apoptosis. Flow cytometric detection of phosphatidylserine expression on early apoptotic cells using fluorescein labelled Annexin V. J Immunol Methods 1995;184:39–51.
[21] De Tomasi JA. Improving the technic of the Feulgen stain. Stain Tech 1936;11:137–44.
[22] Pearse AGE. Histochemistry, theoretical and applied. Boston: Little, Brown & Company; 1980.
[23] Shevach EM. Labeling cells in microtiter plates for determination of [^{3}H] thymidine uptake. In: Coligan JE, Kruisbeek AM, Margulies DH, Shevach EM, Strober W, editors. Current protocols in immunology, vol. 2. New York: Wiley; 1994.
[24] Bradford MM. A rapid and sensitive method for the quantitation of microgram quantities of protein utilizing the principle of protein-dye binding. Anal Biochem 1976;72:248–54.
[25] Sinha BK, Yamazaki H, Eliot HM, Schneider E, Borner MM, O'Connor PM. Relationships between proto-oncogene expression and apoptosis induced by anticancer drugs in human prostate tumor cells. Biochim Biophys Acta 1995;1270:12–8.
[26] Royall JA, Ischeropoulos H. Evaluation of 2′,7′-dichlorofluorescin and dihydrorhodamine as fluorescent probes for intracellular hydrogen peroxide in cultured endothelial cells. Arch Biochem Biophys 1993;302:348–55.
[27] Buege JA, Aust SD. Microsomal lipid peroxidation. Methods Enzymol 1978;52:302–10.
[28] Nagelkerke JF, Dogterom P, De Bont HJGM, Mulder GJ. Prolonged high intracellular free calcium concentrations induced by ATP are not immediately cytotoxic in isolated rat hepatocytes. Biochem J 1989;263:347–53.
[29] Scott DA, Moreno SN, Docampo R. Calcium storage in Trypanosoma brucei: the influence of cytoplasmic pH and the importance of vacuolar acidity. Biochem J 1995;310:784–94.
[30] Ambudkar IS, Kuyatt BL, Roth BS, Baum BJ. Modification of ATP-dependent calcium transport in rat parotid basolateral membranes during aging. Mech Ageing Dev 1988;43:45–60.
[31] Gant TW, Rao DN, Mason RP, Cohen GM. Redox cycling and sulphydryl arylation; their relative importance in the mechanism of quinone cytotoxicity to isolated hepatocytes. Chem Biol Interact 1988;65:157–.
[32] Mirabelli F, Salis A, Vairetti M, Bellomo G, Thor H, Orrenius S. Cytoskeletal alterations in human platelets exposed to oxidative stress are mediated by oxidative and Ca^{2+} dependent mechanisms. Arch Biochem Biophys 1989;270:478–.
[33] Clopton DA, Saltman P. Low-level oxidative stress causes cell-cycle specific arrest in cultured cells. Biochem Biophys Res Commun 1995;210:189–96.
[34] De Laurenzi V, Melino G, Savini I, Annicchiarico-Petruzzelli M, Finazzi-Agrò A, Avigliano L. Cell death by oxidative stress and ascorbic acid regeneration in human neuroectodermal cell lines. Eur J Cancer 1995;31:463–6.
[35] Bellomo G, Mirabelli F, Vairetti M, Iosi F, Mallorni W. Cytoskeleton as a target in menadione-induced oxidative stress in cultured mammalian cells. Biochemical and immunocytochemical features. J Cell Physiol 1990;143:118–28.
[36] Malorni W, Iosi F, Malorni F, Bellomo G. Cytoskeleton as a target in menadione-induced oxidative stress in cultured mammalian cells: alterations underlying surface bleb formation. Chem Biol Interact 1991;80:217–36.
[37] Wartenberg M, Diedershagen H, Hescheler J, Sauer H. Growth stimulation versus induction of cell quiescence by hydrogen peroxide in prostate tumor spheroids is encoded by the duration of the Ca^{2+} response. J Biol Chem 1999;274:27759–67.
[38] Bellomo G, Nicotera P, Orrenius S. Alterations in intracellular calcium compartmentation following inhibition of calcium efflux from isolated hepatocytes. Eur J Biochem 1984;144:19–23.
[39] Bellomo G, Jewell SA, Thor R, Orrenius S. Regulation of intracellular calcium compartmentation: studies with isolated hepatocytes and *t*-butyl hydroperoxide. Proc Natl Acad Sci USA 1982;79:6842–6.
[40] Jamison JM, Gilloteaux J, Taper HS, Buc Calderon P, Summers JL. Autoschizis: a novel cell death. Biochem Pharmacol 2002;63:1773–83.
[41] Buc Calderon P, Cadrobbi J, Marques C, Hong-Ngoc N, Jamison JM, Gilloteaux J, Summers JL, Taper HS. Potential therapeutic application of the association of Vitamins C and K_3 in cancer treatment. Curr Med Chem 2002;9:2269–85.
[42] Chen QM, Liu J, Merrett JB. Apoptosis or senescence-like growth arrest: influence of cell-cycle position, p53, p21 and bax in H_2O_2 response of normal human fibroblasts. Biochem J 2000;347:543–51.
[43] Gelvan D, Moreno V, Clopton DA, Saltman P. Sites and mechanisms of low-level oxidative stress in cultured cells. Biochem Biophys Res Commun 1995;206:421–8.
[44] Chen QM, Tu VC, Catania J, Burton M, Toussaint O, Dilley T. Involvement of Rb family proteins, focal adhesion proteins and protein synthesis in senescent morphogenesis induced by hydrogen peroxide. J Cell Sci 2000;113:4087–97.
[45] Bijur GN, Briggs B, Hitchcock CL, Williams MV. Ascorbic acid, dehydroascorbate induces cell cycle arrest at G_2/M DNA damage checkpoint during oxidative stress. Environ Mol Mutagen 1999;33: 144–52.
[46] Bijur GN, Ariza ME, Hitchcock CL, Williams MV. Antimutagenic and promutagenic activity of ascorbic acid during oxidative stress. Environ Mol Mutagen 1997;30:339–45.
[47] Leung PY, Miyashita K, Young M, Tsao CS. Cytologic effect of ascorbate and its derivatives on cultured malignant and nonmalignant cell lines. Anticancer Res 1993;13:475–80.
[48] Clement MV, Ramalingam J, Long LH, Halliwell B. The *in vitro* cytotoxicity of ascorbate depends on the culture medium used to perform the assay and involves hydrogen peroxide. Antioxid Redox Signal 2001;3:157–63.
[49] Sata N, Klonowski-Stumpe H, Han B, Häussinger D, Niederau C. Menadione induces both necrosis and apoptosis in rat pancreatic acinar AR4-2J cells. Free Radic Biol Med 1997;23:844–50.

[50] Wu FY, Chang NT, Chen WJ, Juan CC. Vitamin K_3-induced cell cycle arrest and apoptotic cell death are accompanied by altered expression of *c-fos* and *c-myc* in nasopharyngeal carcinoma cells. Oncogene 1993;8:2237–44.

[51] Wu FYH, Sun T-P. Vitamin K_3 induces cell cycle arrest and cell death by inhibiting Cdc25 phosphatase. Br J Cancer 1999;35: 1388–93.

[52] McGinn CJ, Miller EM, Lindstrom MJ, Kunugi KA, Johnston PG, Kinsella TJ. The role of cell cycle redistribution in radiosensitization: implications regarding the mechanism of fluorodeoxyuridine radiosensitization. Int J Radiat Oncol Biol Phys 1994;30:851–9.

[53] Sun Y, Oberley LW, Elwell JH, Sierra-Rivera E. Antioxidant enzyme activities in normal and transformed mouse liver cells. Int J Cancer 1989;44:1028–33.

[54] Frei B, England L, Ames BN. Ascorbate is an outstanding antioxidant in human blood plasma. Proc Natl Acad Sci USA 1989;86:6377–81.

[55] Rosin MP, San RHC, Stich HF. Mutagenic activity of ascorbate in mammalian cell cultures. Cancer Lett 1980;8:299–305.

[56] Jarabak R, Jarabak J. Effect of ascorbate on the DT-diaphorase-mediated redox cycling of 2-methyl-1,4-naphthoquinone. Arch Biochem Biophys 1995;318:418–23.

[57] Pething R, Gascoyne PRC, Mc Laughlin JA, Szent-Gyorgi A. Ascorbate-quinone interactions: electrochemical, free radical and cytotoxic properties. Proc Natl Acad Sci USA 1983;80:129–32.

[58] Dypbukt JM, Ankerona M, Burkitt M, Sjöholm Å, Ström K, Orrenius S, Nicotera P. Different prooxidant levels stimulate growth, trigger apoptosis, or produce necrosis of insulin-secreting RINm5F cells. J Biol Chem 1994;269:30553–60.

[59] Laux A, Nel I. Evidence that oxidative stress-induced apoptosis by menadione involves Fas-dependent and Fas-independent pathways. Clin Immunol 2001;101:335–44.

[60] Hampton MB, Orrenius S. Dual regulation of caspase activity by hydrogen peroxide: implications for apoptosis. FEBS Lett 1997;414: 552–6.

[61] Samali A, Nordgren H, Zhivotovsky B, Peterson E, Orrenius S. A comparative study of apoptosis in HepG2 cells: oxidant-induced caspase inactivation leads to necrosis. Biochem Biophys Res Commun 1999;255:6–11.

[62] Maruyama M, Irie S, Sato TA. Morphological changes in the nucleus and actin cytoskeleton in the process of Fas-induced apoptosis in Jurkat T cells. Histochem J 2000;32:495–503.

[63] Taper HS, Jamison JM, Gilloteaux J, Gwin CA, Gordon T, Summers JL. *In vivo* reactivation of DNases in implanted human prostate tumors after administration of Vitamin C/K3 combination. J Histochem Cytochem 2001;49:109–19.

[64] Taper HS. Reversibility of acid and alkaline deoxyribonuclease deficiency in malignant tumor cells. J Histochem Cytochem 1980;29: 1053–60.